



## NEUROSCIENCE

# Intensive exercise ameliorates motor and cognitive symptoms in experimental Parkinson's disease restoring striatal synaptic plasticity

Gioia Marino<sup>1†</sup>, Federica Campanelli<sup>1†</sup>, Giuseppina Natale<sup>1</sup>, Maria De Carluccio<sup>1,2</sup>, Federica Servillo<sup>1</sup>, Elena Ferrari<sup>3</sup>, Fabrizio Gardoni<sup>3</sup>, Maria Emiliana Caristo<sup>4</sup>, Barbara Picconi<sup>5,6</sup>, Antonella Cardinale<sup>1,6</sup>, Vittorio Loffredo<sup>7</sup>, Francesco Crupi<sup>7</sup>, Elvira De Leonibus<sup>7,8</sup>, Maria Teresa Viscomi<sup>9,10</sup>, Veronica Ghiglieri<sup>5,10‡</sup>, Paolo Calabresi<sup>1,10‡\*</sup>

Copyright © 2023 The Authors. Some rights reserved; exclusive licensee American Association for the Advancement of Science. No claim to original U.S. Government Works. Distributed under a Creative Commons Attribution NonCommercial License 4.0 (CC BY-NC).

Intensive physical activity improves motor functions in patients with Parkinson's disease (PD) at early stages. However, the mechanisms underlying the beneficial effects of exercise on PD-associated neuronal alterations have not been fully clarified yet. Here, we tested the hypothesis that an intensive treadmill training program rescues alterations in striatal plasticity and early motor and cognitive deficits in rats receiving an intrastriatal injection of alpha-synuclein ( $\alpha$ -syn) preformed fibrils. Improved motor control and visuospatial learning in active animals were associated with a recovery of dendritic spine density alterations and a lasting rescue of a physiological corticostriatal long-term potentiation (LTP). Pharmacological analyses of LTP show that modulations of N-methyl-D-aspartate receptors bearing GluN2B subunits and tropomyosin receptor kinase B, the main brain-derived neurotrophic factor receptor, are involved in these beneficial effects. We demonstrate that intensive exercise training has effects on the early plastic alterations induced by  $\alpha$ -syn aggregates and reduces the spread of toxic  $\alpha$ -syn species to other vulnerable brain areas.

## INTRODUCTION

Parkinson's disease (PD) is the second most common neurodegenerative disease in the world, and in addition to the classical motor signs, such as bradykinesia, rigidity, and tremor, this disorder causes cognitive and mood changes (1). Unfortunately, the available pharmacological therapies against PD are symptomatic, and at present, no putative disease-modifying drug has been proven effective. Clinical studies suggest that motor symptoms associated with PD can be improved through physical exercise (2–4). Recently, a clinical trial found attenuated motor symptom progression in PD following an aerobic exercise intervention (Park-in-Shape trial) (5). This study shows that aerobic exercise increases functional connectivity of the anterior putamen with the sensorimotor cortex, ameliorates cognitive performances, and reduces global brain atrophy, suggesting a protective action on the corticostriatal sensorimotor network. Moreover, imaging studies in patients with PD report that exercise exerts a modulatory effect on the mesolimbic dopaminergic pathway and increases dopamine (DA) release in the caudate nucleus, suggesting that the beneficial action of exercise

is mediated by corticostriatal plasticity and enhanced DA release (3).

In parallel with these clinical findings, experimental studies in rodent lesion models demonstrate that treadmill improves motor deficits by reducing the loss of DA neurons in the substantia nigra pars compacta (SNpc) (6, 7). Because misfolding and toxic aggregation of  $\alpha$ -synuclein ( $\alpha$ -syn) play a key role in PD pathophysiology (8, 9), the effect of the treadmill has also been investigated in  $\alpha$ -syn-based models. Recent findings in an  $\alpha$ -syn-induced mouse model show that a regular treadmill exercise decreases  $\alpha$ -syn spreading in the brain and protects nigral dopaminergic neurons via the activation of peroxisome proliferator-activated receptor  $\alpha$  in the brain (10). However, the synaptic mechanisms associated with this molecular alteration were not investigated.

Together, clinical and experimental studies converge on the hypothesis that exercise improves both motor and cognitive performances in subjects with mild or moderate disease through experience-dependent neuroplasticity (11). However, a major gap in this field of research is related to understanding the synaptic and molecular mechanisms underlying exercise-induced plastic effects on the striatal synaptic connections and circuits. To address this crucial issue, we have taken advantage of a model induced by bilateral intrastriatal injection of  $\alpha$ -syn preformed fibrils (PFFs) in rats. Using this paradigm at very early stages, it is possible to observe a loss of long-term potentiation (LTP) in striatal spiny projection neurons (SPNs) and abnormal activity of neurons of SNpc associated with motor and behavioral dysfunctions before overt neuronal degeneration (12). In this study, we demonstrate that, when PFFs-injected rats are exposed to an intensive physical training program, striatal LTP is fully expressed, and nigral accumulation of  $\alpha$ -syn aggregates and dendritic spine loss in SPNs are reverted by exercise. With this set of data, we found that intensive

<sup>1</sup>Sezione di Neurologia, Dipartimento di Neuroscienze, Facoltà di Medicina e Chirurgia, Università Cattolica del Sacro Cuore, Rome, Italy. <sup>2</sup>Department of Neurosciences and Neurorehabilitation IRCCS S.Raffaele-Roma, Rome, Italy. <sup>3</sup>Department of Pharmacological and Biomolecular Sciences, University of Milano, Milan, Italy. <sup>4</sup>Cen.Ri.S. Policlinico Gemelli UNICATT, Rome, Italy. <sup>5</sup>Department of Human Sciences and Quality of Life Promotion, Università Telematica San Raffaele, Rome, Italy. <sup>6</sup>IRCCS San Raffaele Roma, Lab. Neurofisiologia Sperimentale, Roma, Italy. <sup>7</sup>Institute of Biochemistry and Cell Biology, National Research Council, Monterotondo (Rome), Italy. <sup>8</sup>Telethon Institute of Genetics and Medicine, Telethon Foundation, Pozzuoli (NA), Italy. <sup>9</sup>Department of Life Science and Public Health, Università Cattolica del Sacro Cuore, Rome, Italy. <sup>10</sup>Fondazione Policlinico Universitario Agostino Gemelli IRCCS, Rome, Italy.

\*Corresponding author. Email: paolo.calabresi@policlinicogemelli.it

†These authors contributed equally to this work.

‡These authors contributed equally to this work.

exercise training has beneficial effects on motor and cognitive performances, both of which were impaired by  $\alpha$ -syn-PFFs. Our results demonstrate the precise striatal synaptic and plastic mechanisms underlying the beneficial effects of exercise on the early stage of PD, further supporting the role of regular motor activity as a critical therapeutic resource in the initial phases of the disease.

## RESULTS

### Setting up of the treadmill exercise trial sessions

We first established an ideal training protocol combining the minimal exposure to treadmill exercise (intensity, duration, and frequency) necessary to produce measurable changes with little signs of distress (i.e., learning to avoid aversive stimuli, compliance to perform the exercise, and adaptation to performance requirements). To this aim, we habituated the animals to the experimental setting and developed a protocol with a series of gradually increasing speed ramps to build a 30-min training session to evaluate the impact of a given amount of exercise on expected PFFs-induced neuronal changes. Four weeks after receiving a bilateral intra-striatal injection of either phosphate-buffered saline (PBS; vehicle) or PFFs, each rat was handled for 1 week on alternate days and exposed three times to the apparatus (Fig. 1).

The new training protocol was defined by selecting a combination of incremental speeds suitable for adult rats with body weight and age that matched that of operated animals. To motivate rats to walk through the treadmill regularly and at a proper speed, the apparatus is equipped with electric grids at the rear of the treadmill lanes to provide an aversive stimulus. To minimize suffering and

discomfort, we set a maximum of three electric shocks at the lowest intensity for each training session.

Each group of operated animals was further divided into "active" and "sedentary" groups, with the former group subjected to 30 min of exercise protocol and the latter placed into the treadmill equipment with individual lanes switched off for the same amount of time. In the end, the data acquired in the 4 weeks of physical activity were evaluated, and a 30-min session was determined as an adequate duration for an exercise training protocol suitable for both PBS- and PFFs-injected groups. After the treadmill exercise session, *in vivo* analysis of behavior and *ex vivo* morphological, molecular, and electrophysiological experiments were performed 24 hours after the last session to assess the effects of exercise.

### Alpha-syn-PFF rats subjected to treadmill exercise show an improvement in motor and cognitive performances

To test the effect of exercise on locomotion and memory deficits in  $\alpha$ -syn-PFF rats, 8 weeks after the surgery animals were first subjected to the grid walking task (12) to evaluate alterations in locomotion and motor coordination. The PFF sedentary group showed increased latency to reach the top of the grid (treatment  $F_{1,20} = 6.9$ ,  $P = 0.015$ ; exercise  $F_{1,20} = 10.07$ ,  $P = 0.004$ ; treatment  $\times$  exercise  $F_{1,20} = 9.9$ ,  $P = 0.005$ ; Fig. 2A) and increased immobility time (treatment  $F_{1,20} = 5.21$ ,  $P = 0.03$ ; exercise  $F_{1,20} = 7.6$ ,  $P = 0.01$ ; treatment  $\times$  exercise  $F_{1,20} = 5.8$ ,  $P = 0.02$ ; Fig. 2A). Histograms show marked increases in the latency to climb and immobility time in parkinsonian rats, with a significant effect of exercise on rescuing these parameters to control values. Representative track plots show immobility spots typical of PFF sedentary rats compared to the PBS or PFF active group. Thus, exercise rescued these motor deficits in the

Downloaded from https://www.science.org at Universita Studi Milano on July 19, 2023

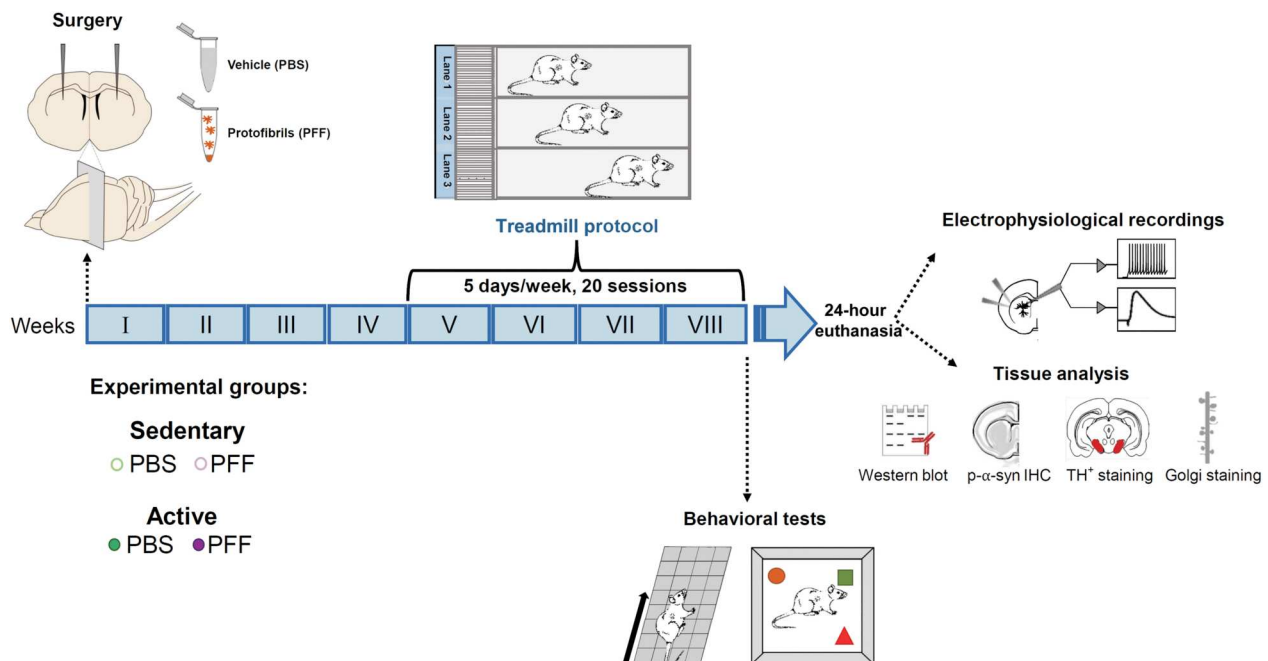


**Fig. 1. Experimental plan.** Schematic representation of the timeline of the experimental procedures and the organization of the experimental groups. Rats were injected with  $\alpha$ -syn-PFFs or PBS at 2 to 3 months. Four weeks after the injection, rats were divided into two groups, sedentary and active. The active animals were enrolled in the treadmill protocol for 4 weeks. Sedentary rats were exposed to an experimental apparatus that was switched off. All experimental groups were then subjected to behavioral tests and used for immunofluorescence, electrophysiological, and other morphological experiments. IHC, immunohistochemistry.

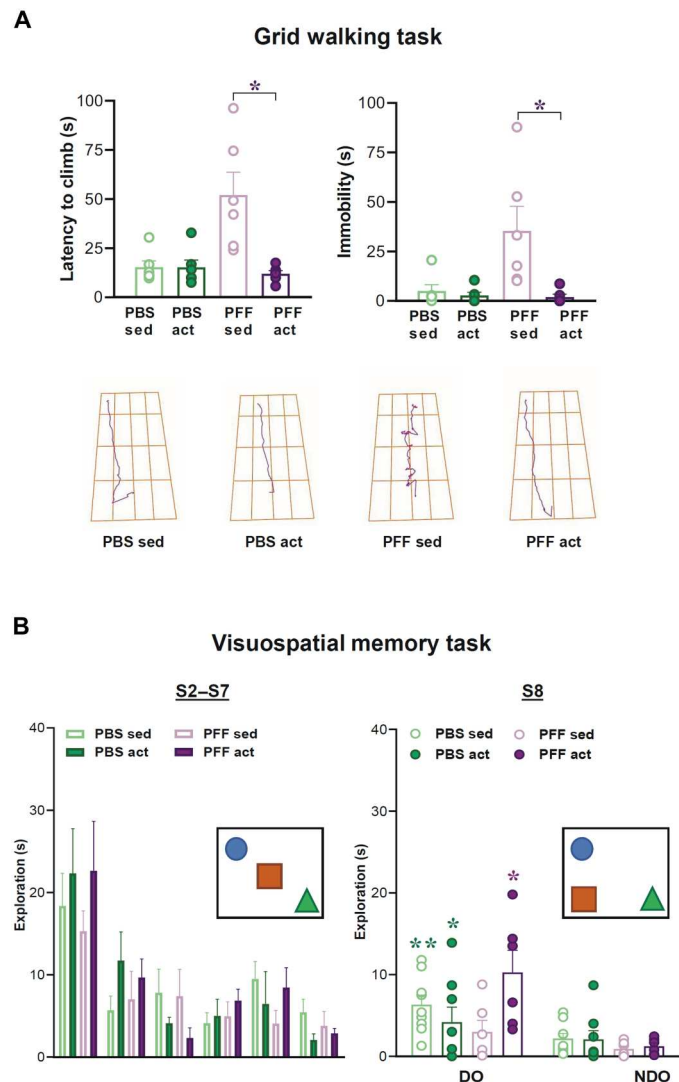


**Fig. 2. Sensorimotor and visuospatial learning in active and sedentary PFFs-injected parkinsonian animals.** (A) Top: Histograms showing averaged and dot plot values of latency to climb (seconds) and immobility time (seconds) in rats injected with PBS or PFFs and subjected to a 4-week treadmill exercise protocol or a sedentary control condition. Bottom: Representative track plots of the trajectory traveled by rats. \* $P < 0.05$ , PFF sed versus all the other groups in the grid test. (B) Left: Histograms illustrating the time (seconds) of object exploration [sessions 2 to 7 (S2 to S7)] during the habituation phase in all experimental groups. Right: Histograms showing the exploration time (seconds) spent exploring a displaced object (DO) and non-displaced objects (NDO) during the session of spatial displacement (S8). Schematic representations of the visuospatial task are reported in the graphs. \* $P < 0.05$ , PFF sed versus all the other groups in the grid test. \*\* $P < 0.01$  PBS sed (DO) versus PBS sed (NDO), \* $P < 0.05$  PBS act (DO) versus PBS act (NDO) and PFF act (DO) versus PFF act (NDO).

PFF group without affecting the behavior of the control groups (\* $P < 0.05$  PFF sed versus PFF act; Fig. 2A).

Bottom panels show a schematic representation of the behavioral procedure used for the visuospatial task (Fig. 2B). Compared to control animals, the PFF sedentary group similarly explored the objects in the arena during the habituation phase, suggesting that novelty reaction and preference were not affected by PFF injection.

Regarding the spatial change, control animals prefer to explore the displaced object (DO) as compared to the non-displaced objects (NDO) (exercise  $F_{1,26} = 7.488$ ,  $P = 0.0110$ ; object exploration  $F_{1,26} = 37.648$ ,  $P = 0.0001$ ; Fig. 2B and fig. S8), while the PFF sedentary group did not. This deficit in spatial novelty discrimination was rescued in the PFF active group, as evidenced by their ability to explore the DO more than the NDO. Exercise training did not modify the spatial behavior in the control group.

### Treadmill reduces $\alpha$ -syn diffusion in SNpc and prevents the reduction of nigrostriatal dopaminergic terminals

In PFF-injected rats ( $n = 6$ ), a significant expression of the pathological form of  $\alpha$ -syn, phosphorylated at the Ser<sup>129</sup> residue (p- $\alpha$ -syn) in dopaminergic neurons of the SNpc, was revealed by tyrosine hydroxylase (TH)/p- $\alpha$ -syn double immunolabeling (Fig. 3A, left), as compared to PBS sedentary and active groups (PBS;  $n = 10$ ) (Student's  $t$  test; PBS versus PFF sed  $t = 5.60$ ,  $df = 14$ , \*\*\* $P < 0.001$ ; Fig. 3A, right). On the other hand, no increase in p- $\alpha$ -syn in the ventral tegmental area (VTA) was observed (Student's  $t$  test; PBS versus PFF sed  $t = 0.02$ ,  $df = 14$ ,  $P > 0.05$ ; Fig. 3A). The region-specific increase in the expression of p- $\alpha$ -syn selective was rescued by exercise in the PFF active group ( $n = 13$ ) (Student's  $t$  test; PFF sed versus PFF act  $t = 4.31$ ,  $df = 17$ , \*\*\* $P < 0.001$ ; Fig. 3A, right).

We then evaluated the dopaminergic cell loss by semiquantitative cell counting of the TH<sup>+</sup> neurons both in the SNpc and the VTA of PBS ( $n = 10$ ) and of PFF-injected sedentary ( $n = 6$ ) and active rats ( $n = 13$ ) (Fig. 3B). Data show a reduction of SNpc neurons in the PFF sedentary group, which was not observed in active animals. However, these changes were not significant (ns) in VTA (SNpc: Student's  $t$  test, PBS versus PFF sed,  $t = 2.90$ ,  $df = 14$ , \* $P < 0.05$ ; PFF sed versus PFF act,  $t = 2.11$ ,  $df = 17$ , \* $P < 0.05$ ; VTA: Student's  $t$  test, PBS versus PFF sed,  $t = 0.23$ ,  $df = 15$ ,  $P > 0.05$ ; PFF sed versus PFF act,  $t = 0.35$ ,  $df = 17$ ,  $P > 0.05$ ; Fig. 3B). Data on SNpc were confirmed by unbiased stereological analysis (Student's  $t$  test; PBS versus PFF sed,  $t = 6.397$ ,  $df = 7$ , \*\*\* $P < 0.001$ ; PFF sed versus PFF act,  $t = 4.627$ ,  $df = 7$ , \*\* $P < 0.01$ ; Fig. 3C), reinforcing the effect of exercise on saving TH<sup>+</sup> neurons from death.

Considering the effects of  $\alpha$ -syn PFFs injection on nigrostriatal dopaminergic terminals in the dorsolateral (DL) and dorsomedial (DM) striatum (12), we checked the effects of treadmill exercise on nigrostriatal dopaminergic terminals. We found that, in  $\alpha$ -syn-PFF-injected animals with treadmill exercise (PFF act), the TH<sup>+</sup> immunofluorescence in the DL and DM striatum was significantly higher than in  $\alpha$ -syn-PFF-injected rats (PFF sed) not exposed to exercise (Student's  $t$  test; DL: PBS versus PFF sed,  $t = 5.457$ ,  $df = 15.70$ , \*\*\* $P < 0.001$ ; PFF sed versus PFF act,  $t = 4.276$ ,  $df = 11$ , \*\* $P < 0.01$ ; DM: PBS sed versus PFF sed,  $t = 4.880$ ,  $df = 19$ , \*\*\* $P < 0.001$ ; PFF sed versus PFF act,  $t = 5.170$ ,  $df = 11$ , \*\* $P < 0.01$ ; Fig. 3D).

No significant difference was found between PBS sedentary and PBS active groups (Student's  $t$  test; PBS sed versus PBS act,  $n = 5$  rats; DL:  $t = 2.10$ ,  $df = 12$ ; DM:  $t = 1.53$ ,  $df = 17$ ;  $P > 0.05$ ), indicating that intensive exercise considerably mitigates the rate of dopaminergic terminal degeneration induced by  $\alpha$ -syn-PFFs injection. Furthermore, to explore the functional integrity of dopaminergic presynaptic terminals, we analyzed the immunostaining intensity of striatal DA transporter (DAT) in the striatum of the different experimental groups. We found that, in  $\alpha$ -syn-PFF-injected animals with treadmill exercise (PFF act), the DAT<sup>+</sup> immunofluorescence in the striatum was significantly higher than in  $\alpha$ -syn-PFF-injected rats not

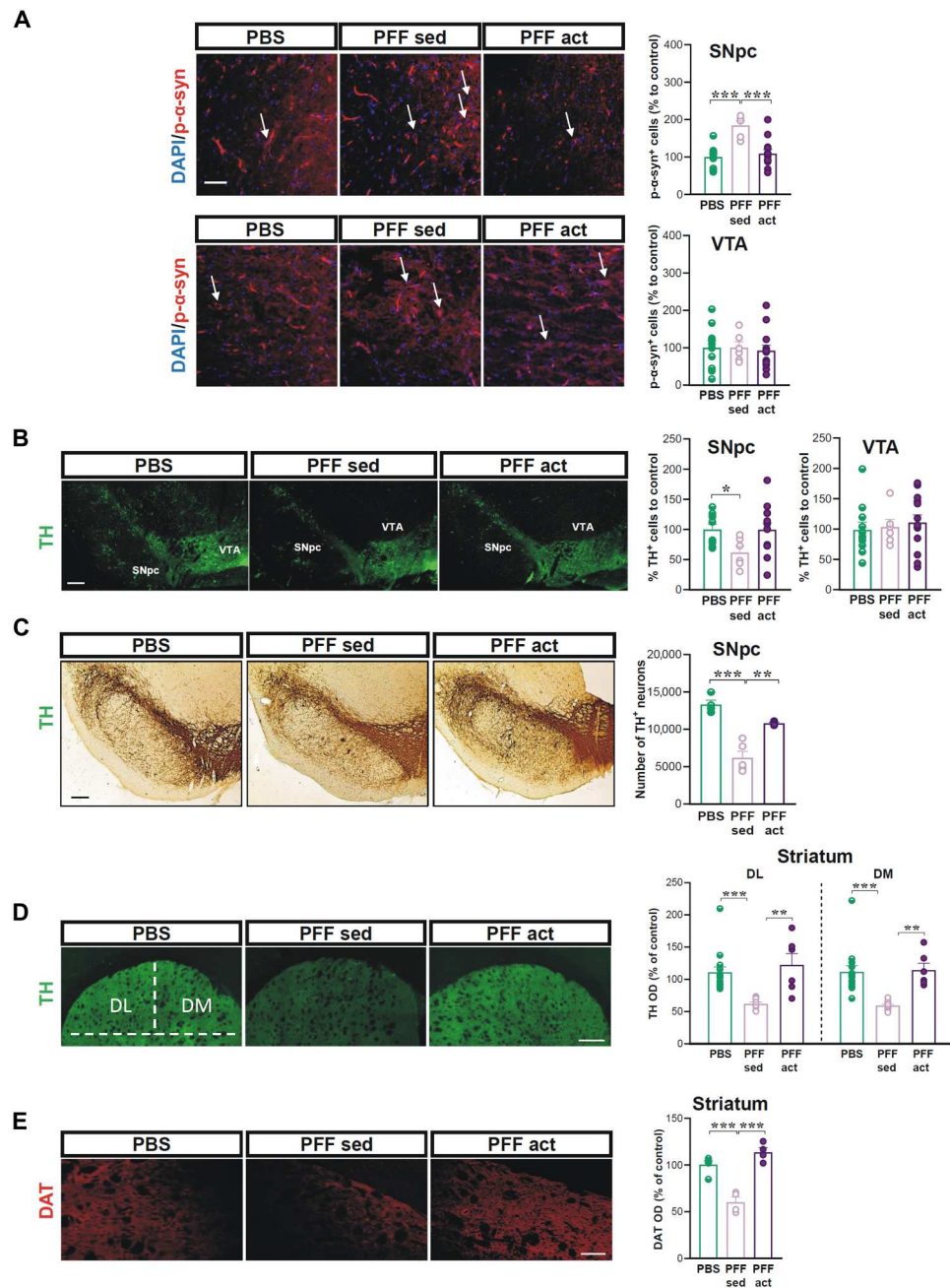


**Fig. 3. Effects of treadmill on  $\alpha$ -syn aggregates diffusion in SNpc and nigrostriatal neurodegeneration.** (A) Left: Representative images at the level of SNpc and VTA showing 4',6-diamidino-2-phenylindole (DAPI) and p- $\alpha$ -syn immunostaining in PBS- and  $\alpha$ -syn-PFF-injected rats, PFF sed, and PFF act, 8 weeks after the injection. White arrows indicate p- $\alpha$ -syn<sup>+</sup> dopaminergic neurons. Scale bar, 100  $\mu$ m. Right: Graphs show the number of p- $\alpha$ -syn<sup>+</sup> cells of the SNpc and VTA. \*\*\* $P$  < 0.001. (B) Representative images (top) at the level of SNpc and VTA in the different experimental groups. Scale bar, 100  $\mu$ m. Graphs (bottom) show the number of TH<sup>+</sup> neurons, % of cells to control, counted in SNpc and VTA in the different experimental groups. \* $P$  < 0.05. (C) Representative images of coronal brain sections showing TH immunoreactivity in the SNpc of the different experimental groups. Scale bar, 200  $\mu$ m. The graph shows the number of TH<sup>+</sup> neurons in the different experimental groups obtained by unbiased stereological analysis. \*\* $P$  < 0.01 and \*\*\* $P$  < 0.001. (D) Representative images of coronal brain sections showing TH immunoreactivity in the dorsolateral (DL) and dorsomedial (DM) portion of the striatum in the different experimental groups. Scale bar, 100  $\mu$ m. The graph shows TH optical density (OD), expressed as a percentage of the control, in both the DL and DM portions of the striatum of the different experimental groups. \*\* $P$  < 0.01 and \*\*\* $P$  < 0.001. (E) Representative images of coronal brain sections at the level of the striatum showing DAT immunoreactivity in the different experimental groups. Scale bar, 50  $\mu$ m. The graph shows DAT OD, expressed as a percentage of the control, in the striatum of the different experimental groups. \*\*\* $P$  < 0.001.

exposed to exercise (PFF sed) and comparable to PBS (Student's *t* test; PBS sed versus PFF sed,  $t = 6.020$ ,  $df = 7$ ,  $***P < 0.001$ ; PFF sed versus PFF act,  $t = 7.225$ ,  $df = 6$ ,  $***P < 0.001$ ; Fig. 3E).

### Corticostriatal plasticity is rescued in response to treadmill exercise training in SPNs of rats injected with $\alpha$ -syn-PFFs

We explored synaptic alterations caused by  $\alpha$ -syn-PFFs by analyzing the ability of SPNs to express LTP in response to a corticostriatal high-frequency stimulation (HFS), a synaptic form of plasticity reflecting the striatal ability of striatal neurons to control motor learning (13, 14). The analysis was then extended to rats subjected to treadmill exercise to evaluate possible beneficial effects of the behavioral paradigm. Ex vivo electrophysiological recordings from corticostriatal slices show that intensive exercise training in PBS-injected rats did not exert detrimental effects on synaptic plasticity, as SPNs of these animals expressed a normal LTP, compared to the PBS sedentary group [paired *t* test pre- versus 20 min post-HFS, PBS sed  $n = 6$ ,  $t = 6.99$ ,  $df = 11$ ; PBS act  $n = 10$ ,  $t = 8.66$ ,  $df = 19$ ;  $***P < 0.001$ ; two-way analysis of variance (ANOVA), group effect  $F_{1,14} = 2.38$ , ns; Fig. 4A].

In contrast, striatal neurons recorded from rats that received an intrastriatal injection of  $\alpha$ -syn-PFFs (PFF sed) did not express this form of synaptic plasticity in response to a HFS protocol (paired *t* test pre- versus 20 min post-HFS, PFF sed  $n = 7$ ,  $t = 0.80$ ,  $df = 13$ , ns; Fig. 4B). A significant effect of exercise was observed in PFF-injected rats subjected to a 4-week treadmill exercise, whose striatal neurons displayed a robust corticostriatal LTP (paired *t* test pre- versus 20 min post-HFS, PFF act  $n = 8$ ,  $t = 7.26$ ,  $df = 15$ ,  $***P < 0.001$ ; two-way ANOVA, interaction group  $\times$  treatment  $F_{28,364} = 6.59$ , group effect  $F_{1,13} = 33.05$ , from 1 to 4 min post-HFS  $***P < 0.05$ , from 5 to 20 min post-HFS  $***P < 0.001$ ; Fig. 4B).

We then explored whether LTP observed in active rats could be depotentiated, a typical property of activity-dependent corticostriatal plasticity under physiological conditions. In a separate set of experiments, we tested the response of the potentiated excitatory postsynaptic potential (EPSP) to a low-frequency stimulation (LFS) protocol (15, 16). In active PFF-injected animals, the restored LTP could be reversed, showing a physiological response to the LFS protocol, as shown in PBS groups (paired *t* test pre- versus 20 min post-HFS, PBS sed  $n = 5$ ,  $t = 7.50$ ,  $df = 9$ ; PBS act  $n = 3$ ,  $t = 9.01$ ,  $df = 5$ ;  $***P < 0.001$ ; paired *t* test pre- versus 20 min post-HFS, PFF act  $n = 6$ ,  $t = 6.05$ ,  $df = 11$ ,  $***P < 0.001$ ; Fig. 4, C and D).

### Exercise exerts a durable recovery of striatal synaptic plasticity in parkinsonian animals

Considering the beneficial effects of intensive exercise on synaptic plasticity, we explored the persistence of LTP 7 days after the last treadmill session in SPNs of  $\alpha$ -syn-PFF rats (Fig. 4E). Striatal neurons recorded from PFF active rats 1 week after exercise withdrawal still displayed a full expression of LTP (paired *t* test pre- versus 20 min post-HFS, PFF act POST 1W  $n = 7$ ,  $t = 5.80$ ,  $df = 13$ ,  $***P < 0.001$ ; two-way ANOVA, interaction group  $\times$  treatment  $F_{28,364} = 0.88$ , PFF act versus PFF act POST 1W, ns; Fig. 4E).

### Pharmacological modulation of exercise-induced LTP in striatal SPNs of $\alpha$ -syn-PFF rats

Because brain-derived neurotrophic factor (BDNF) has been referred to as a biomarker of the beneficial effects of intensive exercise, we investigated whether treadmill exercise could increase striatal

levels of this neurotrophic factor. Western blot analysis of striatal homogenates shows that BDNF levels increase after 4 weeks of exercise training (Fig. 5A).

This increase was significant in both PBS- and PFF-injected rats (unpaired Student's *t* test PBS sed,  $n = 7$ , versus PBS act,  $n = 8$ ,  $t = 2.255$ ,  $df = 13$ ,  $*P < 0.05$ ; PFF sed,  $n = 7$ , versus PFF act,  $n = 8$ ,  $t = 4.681$ ,  $df = 13$ ,  $***P < 0.001$ ; Fig. 5A), indicating that BDNF might be involved in the beneficial effects of treadmill exercise associated with the expression of an LTP in SPNs. Total levels of tropomyosin receptor kinase B (TrkB), the BDNF receptor, did not change (unpaired Student's *t* test PBS sed,  $n = 6$ , versus PBS act,  $n = 7$ ,  $t = 0.3258$ ,  $df = 11$ , ns; PFF sed,  $n = 6$ , versus PFF act,  $n = 8$ ,  $t = 0.8805$ ,  $df = 12$ , ns; Fig. 5B).

We then conducted the experiments to test the hypothesis that increased BDNF could play a role in the recovered LTP observed in active animals via pharmacological manipulation of the striatal TrkB receptor. BDNF-TrkB signaling in striatal neurons controls motor behavior (17), and  $\alpha$ -syn down-regulates BDNF expression and TrkB-dependent activities, triggering dopaminergic cell death in PD (18, 19). On the basis of these considerations, we tested the effect of the BDNF/TrkB pathway inhibitor ANA-12 to explore whether the blockade of this signaling was sufficient to disrupt the effects of exercise. In particular, corticostriatal slices were incubated for 1 hour with ANA-12, before the recording. Under this condition, delivery of HFS in striatal neurons was able to induce a normal LTP in SPNs of PBS-injected sedentary animals (paired *t* test pre- versus 20 min post-HFS,  $n = 7$ ,  $t = 6.99$ ,  $df = 11$ ,  $***P < 0.001$ ; Fig. 5C). Unexpectedly, the same protocol, instead, produced a blockade of this form of synaptic plasticity in the PBS active group (paired *t* test pre- versus 20 min post-HFS, PBS act 3  $\mu$ M,  $n = 7$ ,  $P > 0.05$ ; two-way ANOVA, interaction group  $F_{56,420} = 10.75$ , from 1 to 20 min post-HFS, PBS sed 3  $\mu$ M versus PBS act 3  $\mu$ M and PBS sed versus PBS act, 3  $\mu$ M  $***P < 0.001$ ; Fig. 5C). In line with our hypothesis, TrkB antagonism was able to disrupt the restored induction of LTP in the PFF active group (paired *t* test pre- versus 20 min post-HFS, PFF act 3  $\mu$ M,  $n = 4$ ,  $P > 0.05$ ; two-way ANOVA, interaction group  $F_{28,280} = 5.214$ , from 1 to 20 min post-HFS, PFF sed versus PFF act 3  $\mu$ M,  $***P < 0.001$ ; Fig. 5D). These data suggest that BDNF dependence of LTP, associated with the increase in BDNF levels (Fig. 5A), in addition to rescuing plasticity in the PFF rat model, is a general effect on control animals subjected to intensive exercise.

To explore whether the exercise-induced LTP shares similar features of physiological plasticity and to study its properties, in addition to BDNF dependence, we used a pharmacological approach in testing the effects of DA receptors (D1R and D2R) and *N*-methyl-D-aspartate receptor (NMDAR) subunit (GluN2A and GluN2B) antagonists. Considering that, under physiological conditions, LTP is mediated by D1R and NMDAR activation, we bath applied 10  $\mu$ M SCH-23390, a D1R antagonist, for 10 min before inducing HFS protocol. Results show that the antagonist was able to abolish exercise-induced LTP (paired *t* test pre- versus 20 min post-HFS,  $n = 5$ ,  $P > 0.05$ ; Fig. 5E), confirming the essential role of these receptors in this recovered synaptic plasticity. In contrast, the D2R antagonist, 5  $\mu$ M sulpiride, as expected (20), did not lead to any change (paired *t* test pre- versus 20 min post-HFS,  $n = 5$ ,  $t = 10.63$ ,  $df = 9$ ,  $***P < 0.0001$ ; Fig. 5E), confirming its marginal role in LTP induction and maintenance.

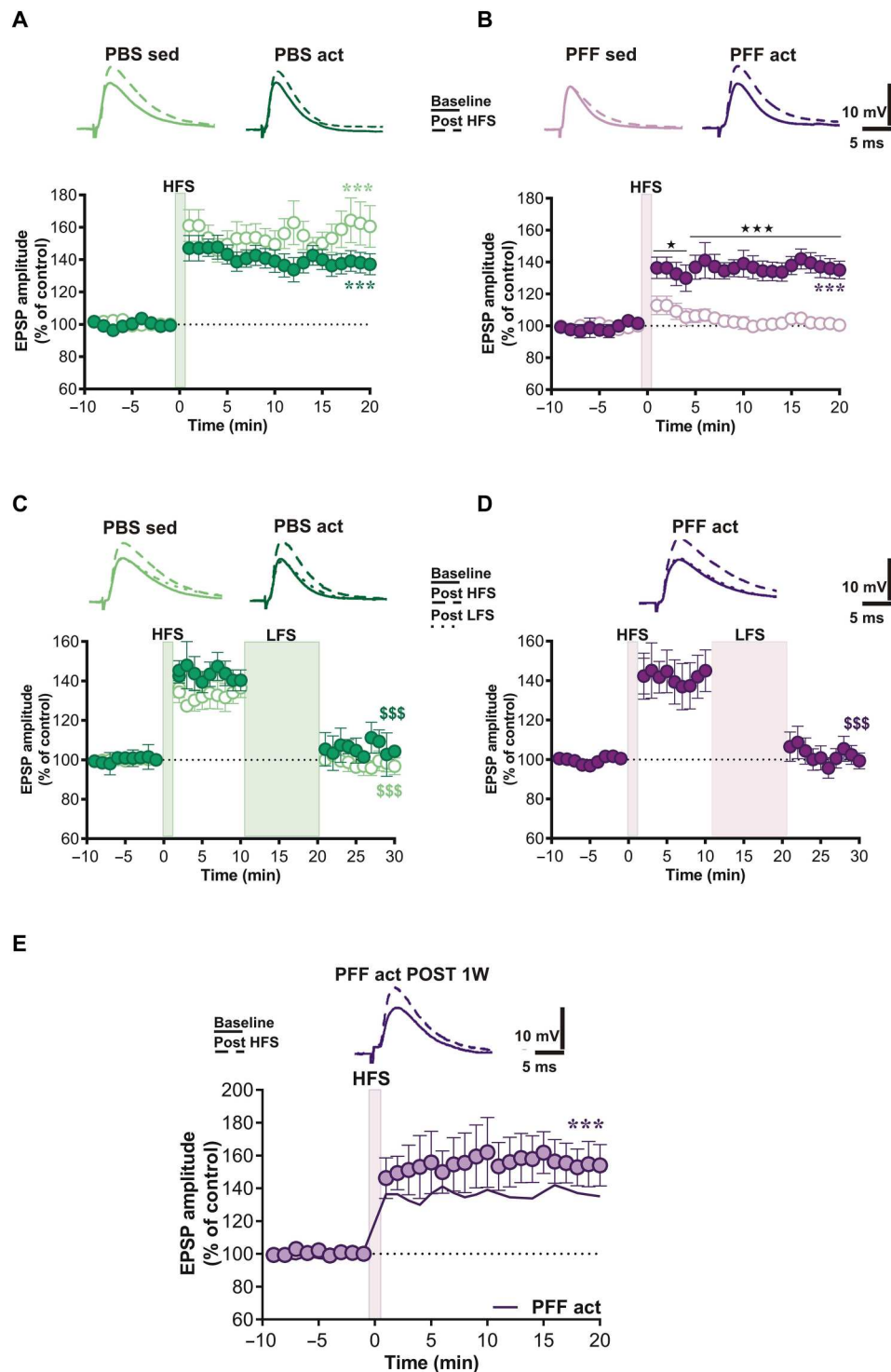


**Fig. 4. Analysis of corticostriatal synaptic plasticity recorded in striatal neurons of PBS- and PFFs-injected active and sedentary animals.** Time course of excitatory postsynaptic potential (EPSP) amplitude in response to an LTP protocol in SPNs recorded from rats subjected to (A) PBS or (B) PFF intrastratial injection and enrolled into a treadmill exercise training protocol. Time course of EPSP amplitude changes recorded in SPNs of (C) PBS- and (D) PFF-injected rats in response to the application of HFS, in the absence of magnesium ions, and a subsequent LFS protocol. Scale bars, 5 ms/10 mV. Top: Representative traces of single SPNs recorded from PBS and PFF groups before (solid lines) and after HFS (dashed lines). (E) Time course of EPSP amplitude in response to LTP protocol in SPNs recorded from PFF rats subjected to treadmill exercise training protocol and after 1 week from the last training session. \* $P < 0.05$ , \*\*\* $P < 0.001$ , and \$\$\$ $P < 0.001$ .

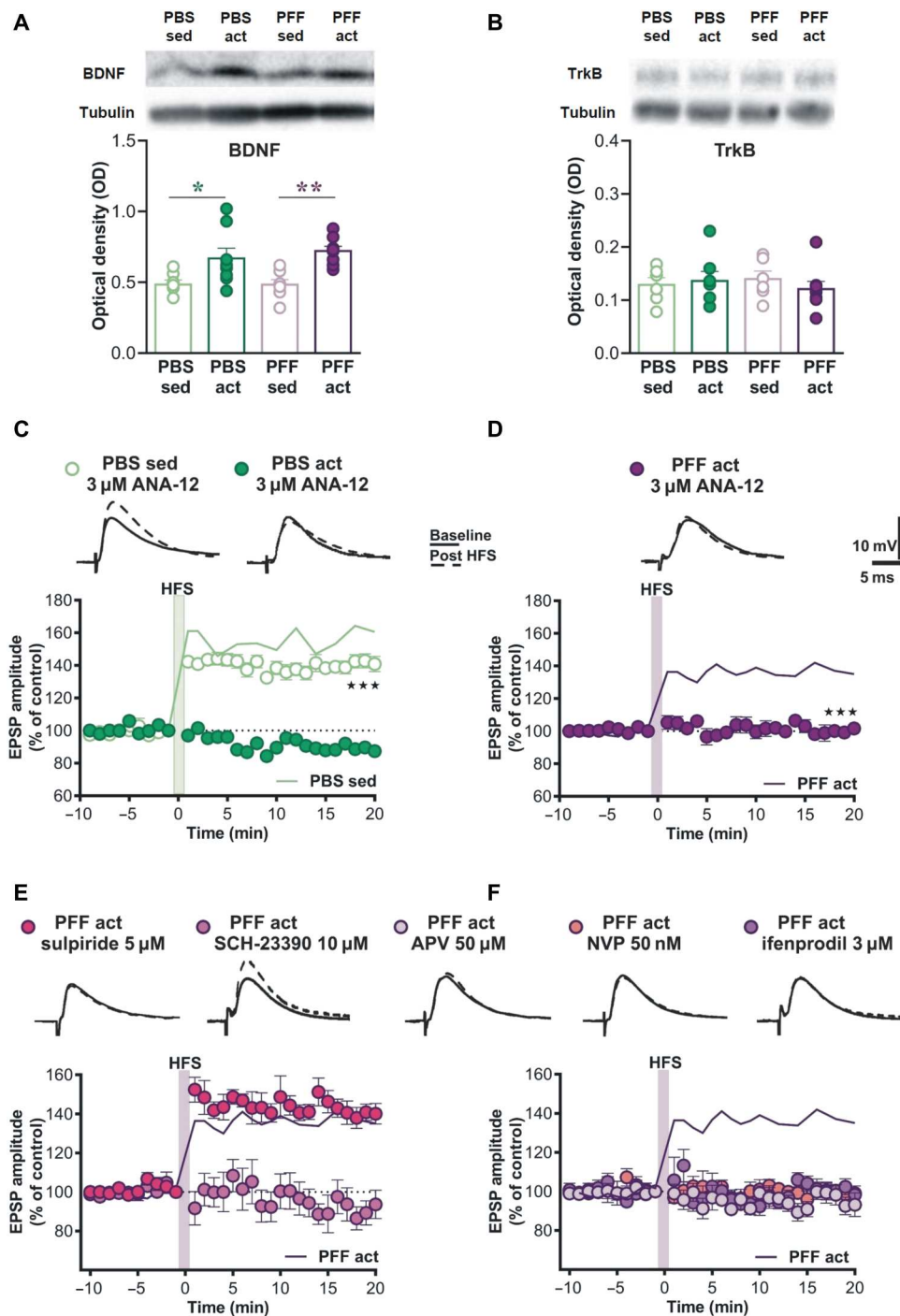


**Fig. 5. Changes in the protein levels of striatal BDNF and involvement of BDNF-TrkB receptor pathway and GluN2B subunits in the exercise-induced LTP. (A and B)** OD representing the BDNF and TrkB levels in striatal homogenates obtained from brain samples of rats injected with either PBS or PFF and then subjected (act) or not (sed) to treadmill exercise training and evaluated by Western blot. **(C and D)** Time course of LTP in striatal SPNs from all experimental groups, recorded after 1 hour of incubation with TrkB inhibitor ANA-12 at the concentration of 3 μM. Time course of LTP in striatal SPNs from the PFF act group, recorded during bath application of **(E)** dopamine receptors (DAR) antagonists (SCH-23390 10 μM and sulpiride 5 μM) and **(F)** NMDAR antagonists (APV 50 μM, NVP 50 nM, and ifenprodil 3 μM). Scale bars, 5 ms/10 mV. Top: Representative traces of single SPNs recorded from PBS and PFF groups before (solid lines) and after HFS (dashed lines).

Downloaded from https://www.science.org at Universita Studi Milano on July 19, 2023

In adult rats under physiological conditions, GluN2A- but not GluN2B-expressing NMDARs are essential for LTP induction (21). Our findings show that bath application of either a broad-spectrum NMDAR (APV 50  $\mu$ M), selective GluN2A (NVP 50 nM), or GluN2B (ifenprodil 3  $\mu$ M) antagonist suppresses the exercise-induced LTP, suggesting that both GluN2A and GluN2B play an essential role in this form of LTP in PFF-injected animals (paired *t* test pre- versus 20 min post-HFS,  $n = 5$  for each drug,  $P > 0.05$ ; Fig. 5F). This latter finding indicates that, unlike under physiological conditions, activation of GluN2B-containing NMDARs in SPNs is essential for the exercise-induced recovery of LTP in parkinsonian animals.

### Exercise induces a full recovery of spine density in striatal SPNs of $\alpha$ -syn-PFF animals

It is well demonstrated that spine formation is an NMDAR-dependent process, and immature spines are particularly enriched in GluN2B-expressing NMDARs (22). We then performed unbiased measurements of dendritic spine density in SPNs of Golgi-stained striata of the different experimental groups. As expected, a significant effect of the PFF injection on SPN spine density was observed ( $n = 4$ ; two-way ANOVA;  $F_{1,12} = 15.055$ ,  $P < 0.01$ ; PBS sed versus PFF sed  $*P < 0.05$ ; Fig. 6, A and B), indicating the disruptive effect of the  $\alpha$ -syn-PFFs injection on dendritic spine features.

Furthermore, we found a significant effect of treatment ( $n = 4$ ; two-way ANOVA;  $F_{1,12} = 13.98$ ,  $P < 0.01$ ; PFF sed versus PFF act  $*P < 0.05$ ; Fig. 6, A and B), with the active group (PFF act) showing a higher spine density compared to the sedentary group (PFF sed). However, the two-way ANOVA did not display a significant effect of injection and treatment (interaction  $F_{1,12} = 0.935$ ;  $P = 0.352$ , ns), with the PFF act group showing a spine density similar to the PBS act group (Fig. 6, A and B), meaning that the intense exercise did not exert changes on the SPN spine density of the PBS group.

Furthermore, as changes in size and shape of synaptic spines are associated with the maturation and stability of synapses, with the thin spines carrying immature synapses and the stubby mature synapses, we measured spine head diameters on SPNs of the different experimental groups. Besides the increased density of spines in SPNs, we found a significant effect of injection on the percentage of thin over the total number of spines, with a significant effect of injection (two-way ANOVA  $F_{1,12} = 9.32$ ,  $P < 0.05$ ; PFF sed versus PBS sed  $**P < 0.01$ ; Fig. 6, A to C), of treatment ( $F_{1,12} = 23.25$ ,  $P < 0.001$ ; PFF sed versus PFF act  $***P < 0.001$ ), and of the interaction (injection  $\times$  treatment  $F_{1,12} = 20.20$ ,  $P < 0.001$ ). No substantial differences in the percentage of mature stubby spines/total spines were observed among groups (Fig. 6, A to D), suggesting that the immature might support the recovery of synaptic plasticity observed in SPNs of PFF act animals.

## DISCUSSION

In the present study, using a progressive and well-characterized  $\alpha$ -syn-based model of early PD, we found that active exercise fully restores corticostriatal striatal LTP that was abolished by the intrastriatal injection of  $\alpha$ -syn-PFFs. In this model of early PD, we observed that this recovery of LTP was durable, because it lasts at least 1 week after the interruption of the treadmill.

The recovery of corticostriatal synaptic plasticity after active exercise has been hypothesized by previous clinical studies. A recent

clinical study in patients with PD found that aerobic exercise increases the functional connectivity of the putamen with the sensorimotor cortex (5). This study reported that exercise also improves cognitive performance control and reduces brain atrophy. Thus, the authors hypothesized that aerobic exercise stimulates functional and structural neuroplasticity in both motor and cognitive brain networks in PD. These findings align with previous data from animal models of PD, where aerobic exercise stimulates protective and restorative effects, possibly via recovery of neuroplasticity in the basal ganglia network (11). However, it should be stressed that, until now, neither preclinical studies nor clinical investigations were able to demonstrate this assumption, showing that active exercise under the parkinsonian condition can induce the recovery of corticostriatal LTP, an essential form of cellular synaptic plasticity of the basal ganglia, showing the molecular mechanisms underlying this recovery.

In the past, we have characterized this model by combining electrophysiological, optogenetic, immunofluorescence, molecular, and behavioral approaches (12, 21). We found that  $\alpha$ -syn reduces NMDAR-mediated synaptic currents and impairs corticostriatal LTP of SPNs of both direct (D1-positive neurons) and indirect (putative D2-positive neurons) pathways. We also reported that intrastriatal injections of  $\alpha$ -syn produce disturbances in visuospatial memory associated with reduced function of the GluN2A NMDAR subunit, indicating that this protein selectively targets this subunit. Moreover, this change was observed in SPNs activated by optical stimulation of either cortical or thalamic glutamatergic afferents. In addition, antibodies targeting  $\alpha$ -syn prevented the loss of LTP and the reduced synaptic localization of GluN2A NMDAR subunit (21). More recently, we reported that the intrastriatal injection of  $\alpha$ -syn-PFFs induces time-dependent electrophysiological and behavioral alterations via a retrograde transmission (12). In particular, even at the early time point (6 weeks), corticostriatal LTP is abolished. This loss of synaptic plasticity is observed before overt neuronal death, and it is rescued by 1-dopa, a precursor of DA, showing that a dysfunctional DA system plays a critical role in the early phases of the disease (12).

In this study, we found that the exercise-induced recovery of corticostriatal LTP was not coupled with changes in the measured intrinsic membrane properties such as current-voltage (*I-V*) relationship, current-driven firing discharge, and spontaneous glutamate-mediated synaptic transmission, suggesting that the rescue of synaptic plasticity is a rather selective event that is not associated with modifications of basal physiological properties. These electrophysiological findings were paralleled by a behavioral amelioration.  $\alpha$ -Syn-PFF rats subjected to treadmill exercise show an improvement in motor and cognitive performances. In particular, we used the grid walking task to evaluate early alterations in locomotion and motor coordination (23). While the PFF sedentary group showed increased latency to reach the top of the grid and increased immobility time, in active PFF rats, these parameters returned to control values.

Visuospatial impairments are typical of early PD and can be accompanied by memory impairment, with an increasing risk for early progression to dementia (24). In our model, we used object recognition as a behavioral procedure to detect visuospatial deficits. Compared to control animals, the PFF sedentary group similarly explored the objects in the arena during the habituation phase. However, regarding the spatial change, control animals preferred



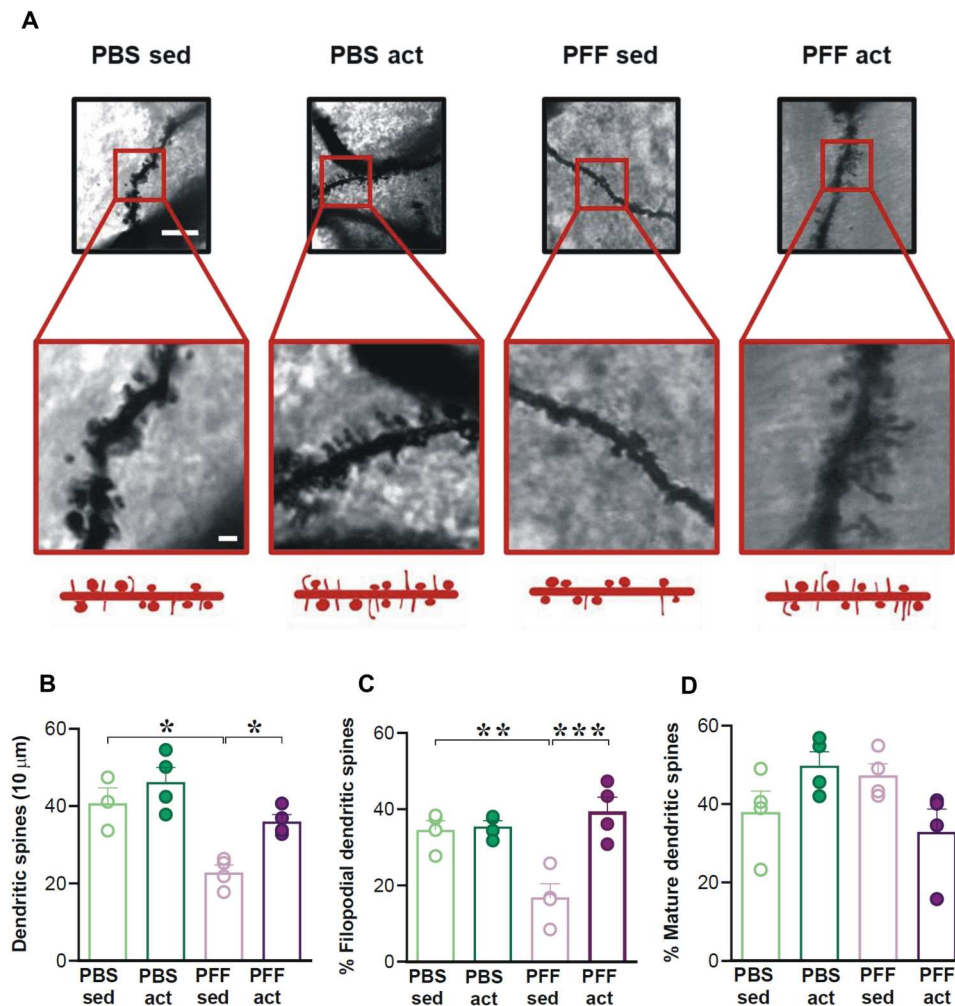


**Fig. 6. Analysis of the spine density on SPNs of PBS- and PFFs-induced sedentary and active rats.** (A) Representative images of Golgi-stained dendritic segments of a striatal SPN in the different experimental groups at lower (top) and higher (bottom) magnifications. Scale bars, 10 μm (top) and 5 μm (bottom). (B) Histograms of the spine density ( $n$  spines per 10 μm) showing the effects of PBS or PFF intraatrial injection and the subsequent effects of sedentary (sed) condition or treadmill (act) protocol on SPN spine density.  $*P < 0.05$ . (C) Histogram showing the quantification of filopodial spines expressed as a percentage of the total number of spines displaying the effects of the different treatments on the immature spines.  $**P < 0.01$  and  $***P < 0.001$ . (D) Histogram showing the amount of mature spines expressed as a percentage of the total number of spines. No substantial effects of PBS or PFF intraatrial injection and of sedentary (sed) or treadmill (act) protocol on mature spines were detected.

the DO as compared to the NDO, while the PFF sedentary group did not. This deficit in spatial novelty discrimination was rescued in the PFF active group, as evidenced by their ability to explore the DO more than NDO, suggesting that exercise is able to correct deficits in visuospatial memory.

Qualitative and quantitative analyses of the immunoreacted material revealed that exercise counteracts  $\alpha$ -syn diffusion to the SNpc and reduces the loss of both TH<sup>+</sup> neurons in SNpc and nigrostriatal terminals, typical of our model. Furthermore, we show that exercise significantly reduced the loss of DAT<sup>+</sup> terminals in the striatum. These findings are of particular interest as they demonstrate the functional integrity of presynaptic terminals onto the striatal medium spiny neurons.

Together, our results support the notion that precocious DA-related deficits are sufficient to produce both behavioral and synaptic alterations, as previously shown (12). In addition, the present data also suggest that exercise, by restoring a physiological striatal

innervation, can rescue DA-dependent LTP, similar to the therapeutic effect of subchronic L-dopa (12). Moreover, the reduction of p- $\alpha$ -syn in SNpc further supports the idea that intensive physical activity, slowing down the nigral diffusion of pathological aggregates, might preserve the functional activity of DA neurons, selectively innervating the DL striatum. The lack of effect of both  $\alpha$ -syn-PFFs and exercise on VTA neurons suggests that, in this early model of PD, neurochemical and plastic changes are specific for motor-related areas.

It has been postulated that exercise might represent an alternative approach to reducing neurodegeneration in PD via the modulation of BDNF (25). Experimental studies show that exercise reduces the loss of DA neurons and movement dysfunction via the activation of the BDNF-TrkB signaling pathway. Similarly, studies on patients with PD show that exercise improves motor performance, increasing BDNF levels and reducing the inflammatory status (2, 26). However, it was unclear whether the beneficial effects

of exercise are mechanistically linked to the reduction of pathological  $\alpha$ -syn species and to the recovery of synaptic plasticity. In our model, we provide strong evidence that the beneficial effects of BDNF increase are associated with the recovery of physiological striatal synaptic plasticity. We report that treadmill exercise increases striatal levels of this neurotrophic factor with no change in the TrkB receptor availability in both control and PFF-injected animals subjected to physical exercise. Moreover, we found that a low micromolar concentration of the BDNF/TrkB pathway inhibitor ANA-12, while it does not affect LTP in sedentary control animals, is able to disrupt this recovered form of plasticity in either PFF-injected or PBS-injected animals that have undergone treadmill. Both these findings strongly support the involvement of BDNF-TrkB signaling in the rescue of SPNs plasticity, also suggesting a possible mechanism for the recovery of motor and visuospatial behavior. Further experiments are required to clarify the permissive role of BDNF on corticostriatal LTP in active control animals. However, our finding is in line with the enhanced BDNF-mediated effects of physical exercise in healthy subjects as a result of a recent meta-analysis of randomized controlled trials (27).

Under physiological conditions, striatal LTP requires the activation of GluN2A- but not GluN2B-bearing NMDARs (21). Unexpectedly, after intensive exercise in PFF-injected parkinsonian animals, we found that, in the recovered LTP, coactivation of GluN2A and GluN2B plays an essential role because the application of GluN2A or GluN2B selective subunit antagonists are both able to suppress the exercise-induced LTP. This finding suggests that these NMDAR subunits might cooperate in recovering synaptic plasticity under specific physiopathological conditions, as we have previously shown in a different experimental model of PD after transcranial magnetic stimulation (22), possibly involving BDNF-TrkB signaling (28). Notably, it has been proposed that, in the induction of the hippocampal LTP, the faster component involves the activation of GluN2A and GluN2B subunits and the slower component involves mainly the activation of GluN2B subunits, while the maintenance phase seems to rely on the activation of NMDARs containing both GluN2A and GluN2B subunits (29). In line with this hypothesis, it has been reported that GluN2A and GluN2B are involved in the function of both synaptic and extrasynaptic NMDARs, demonstrating that they play similar rather than opposing roles in NMDAR-mediated bidirectional regulation of prosurvival signaling and neuronal death (30).

A complex chain of intracellular signaling events, critically important in motor control, is activated by the stimulation of D1-like DA receptors in SPNs. At corticostriatal synapses on SPNs, D1-like receptor-dependent activation of DA and cyclic adenosine 3',5'-monophosphate-regulated phosphoprotein 32 kDa is a crucial step for the induction of LTP that also requires coactivation of NMDARs (13, 31). To verify that exercise-induced LTP has similar pharmacological features, we demonstrated the selective D1 dependence of this form of synaptic plasticity as under physiological conditions. This form of plasticity was also reversed by LFS, further supporting the ability of the treadmill exercise to exert a synaptic therapeutic effect.

In PD, a marked loss of DA underlies complex structural changes in SPNs. In particular, a substantial reduction in striatal dendritic spine density has been shown as a distinctive feature in different rodent models and patients with PD (32, 33). Notably, the synaptic plasticity recovery observed in SPNs of active  $\alpha$ -syn-

PFF-injected animals was also reflected in morphological changes of the dendritic spines. Notably, treadmill exercise after  $\alpha$ -syn-PFFs injection not only significantly increased the SPN spine formation, reaching a level comparable to the PBS-injected groups, but also the new spines were mostly represented by long and immature spines. These findings, in addition to the unchanged density of stubby/mature spines on SPNs of the different groups, suggest that the newly formed spines could be a critical structural component supporting the beneficial effects of exercise training on striatal plasticity.

Our study provides clear evidence that intensive exercise is effective in counteracting  $\alpha$ -syn spreading and in preventing early synaptic deficits, ameliorating motor and cognitive disturbances in parkinsonian animals. For a more comprehensive understanding of the effects of intensive exercise, future experiments should investigate the functional and structural effects of spontaneous motor activity. However, this study has a robust translational implication because it identified mechanisms underlying the therapeutic effects of exercise observed in clinical trials on patients with early PD subjected to an "assisted" treadmill training. From a clinical perspective, these results provide solid experimental support for testing the hypothesis that physical activity also delays PD symptoms in human patients. From a preclinical point of view, this study may foster the research on BDNF-mediated effects with the development of small-molecule TrkB ligands, with agonist or partial agonist profiles to increase the TrkB activity in sedentary parkinsonian rats and decipher the role of BDNF in activity-dependent synaptic plasticity. With this set of data, we shed further light on the  $\alpha$ -syn relationships with other determinants of synaptic plasticity, such as NMDARs, DA signaling, and BDNF/TrkB pathway, revealing that adaptive changes in the striatum can enroll multiple players to build functional, long-lasting changes and structural modifications that reshape striatal connectivity.

## METHODS

### Animals

Two- to 3-month-old Wistar male rats (300 to 350 g) ( $n = 123$ ) were used. All animals were housed four per cage, under a controlled 12-hour light/12-hour dark cycle and temperature (22° to 23°C), with food and water ad libitum. All efforts were made to minimize the number of animals used and their suffering in accordance with the European Directive (2010/63/EU). All procedures have been approved by the Italian Ministry of Health and were conducted in accordance with the national legislation on the use of animals for research and with the Federation of European Laboratory Animal Science Associations guidelines.

### $\alpha$ -Syn protofibril (PFFs) preparation

Lyophilized fresh monomeric  $\alpha$ -syn (0.33 mg) (recombinant human  $\alpha$ -syn) was dissolved in sterile PBS (vehicle) to a final concentration of 1 mg/ml (70  $\mu$ M) for several days at 37°C, with shaking (300 rpm) until samples appeared cloudy. Fibrils were isolated by centrifugation for 30 min at 16,000g. After resuspension in Krebs buffer, the concentration was quantified by subtracting supernatant protein concentration, as determined by  $A_{280}$  (absorbance at 260 nm) absorbance. Fibril formation was confirmed by thioflavin T binding assay and transmission electron microscopy. At the end

of this procedure, the  $\alpha$ -syn-PFFs aliquots were stored at  $-80^{\circ}\text{C}$  until used (21).

### Stereotaxic surgery for $\alpha$ -syn-PFFs injection

Animals anesthetized with a mix of ketamine/xylazine were mounted into a stereotaxic frame and received bilateral injections of either PBS (vehicle) or  $\alpha$ -syn-PFFs in the striatum using a 10- $\mu\text{l}$  Hamilton microsyringe fitted with a 26-gauge steel cannula. The volume injected was 1  $\mu\text{l}$  for each site. The injection rate used was 0.38  $\mu\text{l}/\text{min}$ , and for each site, the cannula was left in place for an additional 2 min before retracting it. The following coordinates were used: anteroposterior, +1.0; mediolateral,  $\pm 3.0$ ; and dorsoventral,  $-5.0$  (21).

### Treadmill exercise training

To avoid a stressful experience, the animals were gradually habituated to the running sessions by exposing them to a slow progression of speed. After several tests, we identified a combination of the intensity and duration of the speed ramps that were associated with no sign of discomfort. Four weeks after receiving an intrastriatal injection of either PBS ( $n = 30$ ) or PFF ( $n = 29$ ), each rat was handled for 1 week on alternate days and exposed three times to the apparatus. At the beginning of the test, animals were placed on the treadmill lane and stimulated to walk for 20 min with increasing speed ramps (starting from 3 to 11 m/min), while the last 10-min ramp at a constant speed (11 m/min). Because we predicted to carry electrophysiological experiments on one animal per day, the protocol was designed with a staggered enrolment of animals (one animal per day to reach a number of four animals per group) into a training period of 4 weeks (five consecutive days a week and 2 days off) (Fig. 1, experimental plan). At the same time, PFF ( $n = 20$ )– and PBS ( $n = 29$ )–injected sedentary animals are also tested under the same experimental conditions but with the rodent treadmill switched off. Each animal was euthanized 1 day (24 hours) after the last (20th) training session, and biological samples were obtained for further analyses and identification of morphological and molecular correlates of behavioral effects of treadmill exercise.

### Visuospatial memory task

Visuospatial memory task was previously described in mice and rats to detect visuospatial impairment in different animal models of PD (34–36). The test consisted of eight sessions (5 min each), with an inter-session interval of 3 min. In session 1 (S1), the arena (60 cm by 60 cm) was empty, while from S2 to S7, rats explored three objects positioned in the arena and acquired information about the objects and their spatial location in the arena (habituation phase). To test spatial novelty discrimination, during the spatial test S8, the objects' configuration was changed by moving one object (the DO) and leaving the other two objects in the same position (NDO; NDO1 and NDO2). Object exploration was defined as the time in which the nose of the animal was directed toward the object ( $<2$ -cm distance). The animals' ability to selectively react to the spatial change was analyzed by calculating the spatial exploration index [DO versus  $\mu$  (NDO1; NDO2)].

### Inclined grid walking task

We tested the sensorimotor performance in  $\alpha$ -syn-PFF–injected rats with respect to control by using the inclined grid walking task, as described in previous works using different rodent

models of PD (12). Briefly, animals were forced to walk on an inclined ( $45^{\circ}$ ) grid (112 cm by 60 cm). The animal was placed downward at the bottom of the inclined grid; the trial ended when the animal reached the top of the grid or when a maximum time of 5 min (300 s) elapsed. The behavior of the animals was recorded by a video-tracking system (ANY-maze, Stoelting, USA), whereby it was possible to subdivide the grid into 16 quads (4 quads by 4 rows). The parameters evaluated were the following: the latency to climb (seconds), defined as the amount of time the animal takes to reach the top of the grid, and the immobility time (seconds), defined as the amount of time in which the animal does not move.

### Immunolabeling in striatum

Rats were euthanized following deep sedation. After sampling, the brains were stored in 4% paraformaldehyde (PFA) (Sigma-Aldrich) at  $4^{\circ}\text{C}$  for at least 24 hours and then passed in a PBS solution with 30% sucrose and 0.02% sodium azide and stored at  $4^{\circ}\text{C}$  for at least 24 hours or until slicing. Slices (30  $\mu\text{m}$ ) were obtained using a cryostat (Leica CM1900) and stored in PBS with 0.02% sodium azide at  $4^{\circ}\text{C}$  for histological procedures.

Striatal sections were incubated with the primary antibody, including mouse TH (1:1000; Millipore, MAB318) and rat anti-DAT (1:600; Sigma-Aldrich, #MAB 369). Then, the sections were incubated for 2 hours with the secondary antibody, including donkey anti-mouse Alexa Fluor 488 and donkey anti-rat Alexa Fluor 555. Neuronal cells were counterstained with 4',6-diamidino-2-phenylindole. Striatal images were acquired using a confocal microscope (LARGE IMAGE 5  $\times$  3 fields acquisition using a  $\times 20$  objective under Nikon confocal microscope NIKON TiE2). Quantification of TH levels was performed on the  $\times 20$  images by densitometric analysis. Striatal TH immunoreactivity, expressed as optical density (OD) units, was measured in the DL and DM striatum on six regularly spaced 30- $\mu\text{m}$  sections (corresponding approximately to bregma +1.8, +1.56, +1.32, +1.08, +0.84, and +0.60 mm) (six sections per animal;  $n = 5/6$  animals per group). Quantification of DAT levels was performed on the  $\times 20$  images by densitometric analysis. Striatal DAT immunoreactivity, expressed as OD, was measured in the DL striatum on six regularly spaced 30- $\mu\text{m}$  sections. Data collecting for densitometry was done by the experimenter blind to the group analyzed.

### Immunolabeling in SNpc and VTA

After sampling, the ventral part of the brain of each animal was stored in 4% PFA (Sigma-Aldrich) at  $4^{\circ}\text{C}$  for at least 24 hours. Then, brains were moved to a 1 $\times$  PBS solution with 30% sucrose and 0.02% sodium azide and stored at  $4^{\circ}\text{C}$  for at least 24 hours or until the slicing procedure. Thirty-micrometer coronal slices were obtained using a cryostat (Leica CM1900) and stored in 1 $\times$  PBS with 0.02% sodium azide at  $4^{\circ}\text{C}$  until the following histological procedures.

A double immunolabeling experiment was performed using antibodies against TH and p- $\alpha$ -Syn to evaluate the presence of the aggregates in the dopaminergic neurons of the SNpc and VTA and to count the number of TH<sup>+</sup> cells. Considering the anteroposterior extent of the SNpc and the VTA, free-floating coronal brain slices were chosen for each animal. After three washes in 1 $\times$  PBS, slices were permeabilized with a 1 $\times$  PBS solution with 0.1% Triton X-100 (Sigma-Aldrich) and 10% normal goat serum (NGS). After 20 min, slices were blocked for 1 hour with a 1 $\times$  PBS solution with 0.1%

Triton X-100, 10% NGS, and 0.1% bovine serum albumin. Primary antibodies of mouse TH (1:1000; MAB318, Merck Millipore) in combination with rabbit hu- $\alpha$ -Syn phosphorylated at Ser<sup>129</sup> (phospho-S129-hu- $\alpha$ -Syn; 1:100; ab51253, Abcam) were applied overnight at 4°C. After three washes with 1× PBS, brain slices were incubated for 2 hours at room temperature with the proper mixture of secondary antibodies: goat anti-rat fluorescein-conjugated (1:300; AP136F, Merck Millipore), goat anti-rabbit Alexa Fluor 568 (1:300; ab175470, Abcam), and goat anti-mouse Alexa Fluor 488 (1:300; AP124JA4, Merck Millipore). Twenty times magnification TH/p- $\alpha$ -syn immunolabeling images were acquired using a Leica DM6000B/M fluorescence upright microscope and Leica Application Suite (LAS-X) software. TH<sup>+</sup> and p- $\alpha$ -syn<sup>+</sup> cells in the SNpc and the VTA were manually counted using ImageJ software (National Institutes of Health, Bethesda, MD) in all the selected slices and averaged for each animal. Considering the anteroposterior extent, the resulting values per animal were normalized on PBS average.

### Immunohistochemistry and stereological analysis in SNpc

For TH immunohistochemistry, primary and secondary antibody solutions as well as ExtrAvidin solutions were prepared in phosphate buffer (PB) and 0.3% Triton X-100. Each incubation step was followed by three 5-min rinses in PB. Sections were incubated 48 hours at 4°C in a solution with a mouse anti-TH antibody (1:1000; MAB318, Merck Millipore) and then incubated for 2 hours with a biotinylated goat anti-mouse antibody (1:200; B-7264, Sigma-Aldrich). Furthermore, sections were incubated for 1 hour in an ExtrAvidin solution (1:500; E2886, Sigma-Aldrich). As chromogen, peroxidase was used (SK-4105, Vector). Last, sections were mounted on chromalin-coated slides, air-dried, dehydrated, and coverslipped. Four animals per group were used for stereological analysis that was performed on brain sections containing the SNpc. Using the Stereo Investigator System (MicroBrightField Europe e.K., Magdeburg, Germany), a three-dimensional optical fractionator counting probe (*x*, *y*, and *z* dimensions of 50  $\mu$ m by 50  $\mu$ m by 20  $\mu$ m, respectively) was applied to obtain unbiased estimates of total TH<sup>+</sup> cells according to published procedures (37). Data collecting for stereology was done by the experimenter blind to the group analyzed.

### Golgi staining

After perfusion, brains were divided into two hemispheres, one of which was dissected into two parts to be processed. After sampling, brains were rapidly rinsed in Milli-Q water and then impregnated accordingly to the FD Rapid GolgiStain Kit manufacturer's instruction (FD NeuroTechnologies Inc.). In completed Golgi-Cox staining, 150  $\mu$ m of coronal slices was obtained through a cryostat (Leica CM1900). Dendritic spine density, filopodia, and stubby spines were analyzed using Neurolucida software (MBF Bioscience) and then calculated from pooled values (10 dendrites per animal). Images were obtained with a  $\times$ 100 immersion oil objective.

To standardize dendritic spine density estimation because of different sizes, the total number of characterized spines has been divided by the total number of dendrites analyzed (starting from proportion upon 10  $\mu$ m). Filopodial and mature spine (stubby within mushroom) percentages have been calculated upon the total number of detailed spines.

### Striatal homogenate preparation and Western blotting

Striatal areas were carefully isolated and collected on dry ice from brain samples from rats injected with either PBS or  $\alpha$ -syn-PFFs. Striatal areas were then homogenized with a Teflon glass potter in ice-cold buffer containing 320 mM sucrose, 1 mM Hepes, 1 mM MgCl<sub>2</sub>, 1 mM NaHCO<sub>3</sub>, and 0.1 mM phenylmethyl sulphonyl fluoride at pH 7.4 in the presence of cOmplete protease inhibitor cocktail tablets (Roche Diagnostics) and PhosSTOP phosphatase inhibitor (Roche Diagnostics). To assess the total levels of BDNF and TrkB, homogenates were denatured with Laemmli buffer and subsequent heating (10 min, 98°C). Twenty to 25  $\mu$ g of proteins was separated onto an 8 to 12% acrylamide/bisacrylamide gel. Proteins were blotted onto a nitrocellulose membrane (Bio-Rad) and probed with the appropriate primary antibodies, followed by the corresponding horseradish peroxidase-conjugated secondary antibodies. Labeling detection was performed with ChemiDoc MP Imaging System (Bio-Rad), and images were acquired with ImageLab software (Bio-Rad). The primary antibodies used in this study were anti-BDNF (1:1000; #329-100, Icosagen) and anti-TrkB (1:1000; #4603, Cell Signaling Technology).

### Ex vivo electrophysiological recordings

The animals used for electrophysiological experiments were divided into four groups: PBS sedentary (*n* = 15), PBS active (*n* = 18), PFF sedentary (*n* = 10), and PFF active (*n* = 34). Corticostriatal coronal brain slices were cut (thickness, 240 to 280  $\mu$ m) using a vibratome (Leica) and incubated in Krebs solution containing 126 mM NaCl, 2.5 mM KCl, 1.2 mM NaH<sub>2</sub>PO<sub>4</sub>, 2.4 mM CaCl<sub>2</sub>, 10 mM glucose, and 25 mM NaHCO<sub>3</sub>. Then, individual slices were transferred into recording chambers continuously perfused with Krebs solution (room temperature; 2.5 to 3 ml/min) saturated with 95% O<sub>2</sub> and 5% CO<sub>2</sub>. Glutamatergic EPSPs were evoked by a bipolar electrode every 10 s, connected to a stimulation unit (Grass Telefactor), and placed within the white matter between the cortex and the striatum to activate glutamatergic fibers. Under this condition, HFS protocol, characterized by three trains (3-s duration, 100 Hz, at 2-s intervals), induced LTP synaptic plasticity (38). EPSP modifications induced by HFS were expressed as a percentage of the mean responses recorded during a stable period (10 min) before tetanus. To reverse a previously induced LTP to baseline values and induce a synaptic depotentiation, a LFS protocol was applied 10 min after LTP induction (2-Hz frequency, 10-min duration), and EPSP responses were observed for at least 10 min. *I-V* relationships and firing rate were obtained by applying steps of current of 100 pA in both hyperpolarizing and depolarizing direction (from -400 to +800 pA, *I-V* curves show steps from -400 to +200 pA) to measure the membrane's ability to accommodate and fire in response to hyperpolarizing and depolarizing current steps. Firing frequency was calculated as a mean number of spikes in response to a step eliciting a maximum response and shown as average in whisker plots.

For intracellular recordings, sharp electrodes were filled with 2 M KCl (30 to 60 megohm). Signals were displayed on a separate oscilloscope, recorded using an Axoclamp 2B amplifier (Molecular Devices), and analyzed on a digital system (pClamp 9, Molecular Devices). Whole-cell patch-clamp recordings were performed on SPNs in the DL striatum and visualized by infrared differential interference contrast microscopy (Eclipse FN1, Nikon) (39). Signals were acquired using Axon Digidata 1550 (Axon Instruments), recorded, and stored on PC using pClamp 10.5 (Molecular

Devices). Recordings, in current-clamp mode, were obtained with a Multiclamp 700B amplifier (Molecular Devices) using borosilicate glass pipettes (outer diameter, 1.5 mm; inner diameter, 0.86 mm) filled with intracellular solution: 120 mM K-gluconate, 0.1 mM  $\text{CaCl}_2$ , 2 mM  $\text{MgCl}_2$ , 0.1 mM EGTA, 10 mM Hepes, 0.3 mM Na-guanosine triphosphate, and 2 mM Mg-adenosine triphosphate, adjusted to pH 7.3 with KOH. Pipette resistances ranged from 6 to 10 megohm. Throughout the experiment, membrane currents were continuously monitored, and access resistance measured in voltage clamp was 15 to 35 megohm before electronic compensation (60 to 80% routinely used). Variations of these parameters (>20%) lead to the exclusion of the experiment. To study spontaneous excitatory postsynaptic currents, patch-clamp electrodes were filled with intracellular solution. Picrotoxin 50  $\mu\text{M}$  (Sigma-Aldrich) was continuously added in all the experiments to block  $\gamma$ -aminobutyric acid type A currents. Slices were preincubated in the presence of different doses of ANA-12, a TrkB inhibitor, for 1 hour. Cells were clamped at the holding potential of  $-70$  mV. Input resistance and injected currents were monitored during the experiments. ANA-12 and picrotoxin were purchased from Sigma-Aldrich (Milan, Italy). Then, dopaminergic D1R and D2R antagonists (SCH 23390 10  $\mu\text{M}$  and sulpiride 5  $\mu\text{M}$ ) and GluN2A and GluN2B subunit antagonists (APV 50  $\mu\text{M}$ , NVP 50 nM, and ifenprodil 3  $\mu\text{M}$ ) were used to understand which of these receptors contributed to the induction of exercise-induced LTP.

### Sample size calculation and statistical analysis Electrophysiological experiments

Analysis of data was performed offline using Clampfit10 (Molecular Devices) and GraphPad Prism. Changes in EPSP amplitude induced by drugs or by stimulation protocols were expressed as a percentage of the baseline, the latter representing the normalized EPSP mean amplitude acquired during a stable period (10 to 15 min) before delivering drugs or stimulation. LTP amplitude was compared using Student's *t* test for paired samples by comparing in each experiment values of the EPSP amplitudes at 20 min post-HFS protocol relative to baseline. Statistical comparisons of the EPSP mean amplitude over time between different experimental groups were analyzed using a two-way ANOVA. *I-V* curves were compared using two-way ANOVA. The significance level was set at  $P < 0.05$ .

### Western blot experiments

One-way ANOVA followed by Tukey's post hoc test or by unpaired Student's *t* test was used as appropriate.

### Morphological (Golgi-based spine scores) measurements

All experimental groups were compared by means of two-way ANOVA by Bonferroni's post hoc test.

### Behavioral analysis

Data were analyzed using two-way ANOVA with treatment (two levels: PBS and PFF) and exercise (two levels: sed and act), using repeated measures for object exploration [DO and  $\mu$  (NDO1; NDO2) for S8]. An appropriate post hoc analysis was used when necessary.

### Cell counting

The number of TH<sup>+</sup> cells per slice was averaged per animal, and data were normalized (considering the SNpc and the VTA anteroposterior extent) on PBS average. For TH<sup>+</sup> fibers in the striatum (DL and DM), data were presented as means  $\pm$  SEM of the OD as a percentage of the control. Unpaired Student's *t* test was used.

## Supplementary Materials

### This PDF file includes:

Supplementary Text  
Figs. S1 and S2  
References

[View/request a protocol for this paper from Bio-protocol.](#)

## REFERENCES AND NOTES

- W. Poewe, K. Seppi, C. M. Tanner, G. M. Halliday, P. Brundin, J. Volkman, A.-E. Schrag, A. E. Lang, Parkinson disease. *Nat. Rev. Dis. Primers* **3**, 17013 (2017).
- M. Schenkman, C. G. Moore, W. M. Kohrt, D. A. Hall, A. Delitto, C. L. Comella, D. A. Josbeno, C. L. Christiansen, B. D. Berman, B. M. Kluger, E. L. Melanson, S. Jain, J. A. Robichaud, C. Poon, D. M. Corcos, Effect of high-intensity treadmill exercise on motor symptoms in patients with de novo parkinson disease: A phase 2 randomized clinical trial. *JAMA Neurol.* **75**, 219–226 (2018).
- M. A. Sacheli, J. L. Neva, B. Lakhani, D. K. Murray, N. Vafai, E. Shahinfard, C. English, S. McCormick, K. Dinelle, N. Neilson, J. McKenzie, M. Schulzer, D. C. McKenzie, S. Appel-Cresswell, M. J. McKeown, L. A. Boyd, V. Sossi, A. J. Stoessl, Exercise increases caudate dopamine release and ventral striatal activation in Parkinson's disease. *Mov. Disord.* **34**, 1891–1900 (2019).
- N. M. van der Kolk, N. M. de Vries, R. P. C. Kessels, H. Joosten, A. H. Zwinderman, B. Post, B. R. Bloem, Effectiveness of home-based and remotely supervised aerobic exercise in Parkinson's disease: A double-blind, randomised controlled trial. *Lancet Neurol.* **18**, 998–1008 (2019).
- M. E. Johansson, I. G. M. Cameron, N. M. Van der Kolk, N. M. de Vries, E. Klimars, I. Toni, B. R. Bloem, R. C. Helmich, Aerobic exercise alters brain function and structure in parkinson's disease: A randomized controlled trial. *Ann. Neurol.* **91**, 203–216 (2022).
- J.-H. Koo, Y.-C. Jang, D.-J. Hwang, H.-S. Um, N.-H. Lee, J.-H. Jung, J.-Y. Cho, Treadmill exercise produces neuroprotective effects in a murine model of Parkinson's disease by regulating the TLR2/MyD88/NF- $\kappa$ B signaling pathway. *Neuroscience* **356**, 102–113 (2017).
- M.-S. Shin, T.-W. Kim, J.-M. Lee, E.-S. Ji, B.-V. Lim, Treadmill exercise alleviates nigrostriatal dopaminergic loss of neurons and fibers in rotenone-induced Parkinson rats. *J. Exerc. Rehabil.* **13**, 30–35 (2017).
- M. G. Spillantini, M. L. Schmidt, V.-M. Lee, J. Q. Trojanowski, R. Jakes, M. Goedert,  $\alpha$ -Synuclein in Lewy bodies. *Nature* **388**, 839–840 (1997).
- G. Marino, P. Calabresi, V. Ghiglieri, Alpha-synuclein and cortico-striatal plasticity in animal models of Parkinson disease. *Handb. Clin. Neurol.* **184**, 153–166 (2022).
- D. Dutta, R. K. Paidi, S. Raha, A. Roy, S. Chandra, K. Pahan, Treadmill exercise reduces  $\alpha$ -synuclein spreading via PPAR $\alpha$ . *Cell Rep.* **40**, 111058 (2022).
- G. M. Petzinger, B. E. Fisher, S. McEwen, J. A. Beeler, J. P. Walsh, M. W. Jakowec, Exercise-enhanced neuroplasticity targeting motor and cognitive circuitry in Parkinson's disease. *Lancet Neurol.* **12**, 716–726 (2013).
- A. Tozzi, M. Sciacaluga, V. Loffredo, A. Megaro, A. Ledonne, A. Cardinale, M. Federici, L. Bellingacci, S. Paciotti, E. Ferrari, A. La Rocca, A. Martini, N. B. Mercuri, F. Gardoni, B. Picconi, V. Ghiglieri, E. De Leonibus, P. Calabresi, Dopamine-dependent early synaptic and motor dysfunctions induced by  $\alpha$ -synuclein in the nigrostriatal circuit. *Brain* **144**, 3477–3491 (2021).
- P. Calabresi, B. Picconi, A. Tozzi, V. Ghiglieri, M. Di Filippo, Direct and indirect pathways of basal ganglia: A critical reappraisal. *Nat. Neurosci.* **17**, 1022–1030 (2014).
- N. Giordano, A. Iemolo, M. Mancini, F. Cacace, M. De Risi, E. C. Latagliata, V. Ghiglieri, G. C. Bellenchi, S. Puglisi-Allegra, P. Calabresi, B. Picconi, E. De Leonibus, Motor learning and metaplasticity in striatal neurons: Relevance for Parkinson's disease. *Brain* **141**, 505–520 (2018).
- V. Ghiglieri, D. Mineo, A. Vannelli, F. Cacace, M. Mancini, V. Pendolino, F. Napolitano, A. di Maio, M. Mellone, J. Stanic, E. Tronci, C. Fidalgo, R. Stancampiano, M. Carta, P. Calabresi, F. Gardoni, A. Usiello, B. Picconi, Modulation of serotonergic transmission by eltopazine in L-DOPA-induced dyskinesia: Behavioral, molecular, and synaptic mechanisms. *Neurobiol. Dis.* **86**, 140–153 (2016).
- B. Picconi, D. Centonze, K. Hakansson, G. Bernardi, P. Greengard, G. Fisone, M. A. Cenci, P. Calabresi, Loss of bidirectional striatal synaptic plasticity in L-DOPA-induced dyskinesia. *Nat. Neurosci.* **6**, 501–506 (2003).
- D. Besusso, M. Geibel, D. Kramer, T. Schneider, V. Pendolino, B. Picconi, P. Calabresi, D. M. Bannerman, L. Minichiello, BDNF-TrkB signaling in striatopallidal neurons controls inhibition of locomotor behavior. *Nat. Commun.* **4**, 2031 (2013).
- Y. Yuan, J. Sun, M. Zhao, J. Hu, X. Wang, G. Du, N.-H. Chen, Overexpression of  $\alpha$ -synuclein down-regulates BDNF expression. *Cell. Mol. Neurobiol.* **30**, 939–946 (2010).

19. S. S. Kang, Z. Zhang, X. Liu, F. P. Manfredsson, M. J. Benskey, X. Cao, J. Xu, Y. E. Sun, K. Ye, TrkB neurotrophic activities are blocked by  $\alpha$ -synuclein, triggering dopaminergic cell death in Parkinson's disease. *Proc. Natl. Acad. Sci. U.S.A.* **114**, 10773–10778 (2017).
20. D. Centonze, B. Picconi, P. Gubellini, G. Bernardi, P. Calabresi, Dopaminergic control of synaptic plasticity in the dorsal striatum. *Eur. J. Neurosci.* **13**, 1071–1077 (2001).
21. V. Durante, A. de Lure, V. Loffredo, N. Vaikath, M. De Risi, S. Paciotti, A. Quiroga-Varela, D. Chiasserini, M. Mellone, P. Mazzocchetti, V. Calabrese, F. Campanelli, A. Mechelli, M. Di Filippo, V. Ghiglieri, B. Picconi, O. M. El-Agnaf, E. De Leonibus, F. Gardoni, A. Tozzi, P. Calabresi, Alpha-synuclein targets GluN2A NMDA receptor subunit causing striatal synaptic dysfunction and visuospatial memory alteration. *Brain* **142**, 1365–1385 (2019).
22. G. Natale, A. Pignataro, G. Marino, F. Campanelli, V. Calabrese, A. Cardinale, S. Pelucchi, E. Marcello, F. Gardoni, M. T. Viscomi, B. Picconi, M. Ammassari-Teule, P. Calabresi, V. Ghiglieri, Transcranial magnetic stimulation exerts "Rejuvenation" effects on cortico-striatal synapses after partial dopamine depletion. *Mov. Disord.* **36**, 2254–2263 (2021).
23. A. Aniszewska, J. Bergström, M. Ingelsson, S. Ekmark-Lewén, Modeling Parkinson's disease-related symptoms in alpha-synuclein overexpressing mice. *Brain Behav.* **12**, e2628 (2022).
24. D. Aarsland, L. Batzu, G. M. Halliday, G. J. Geurtsen, C. Ballard, K. Ray Chaudhuri, D. Weintraub, Parkinson disease-associated cognitive impairment. *Nat. Rev. Dis. Primers.* **7**, 47 (2021).
25. M. Xu, J. Zhu, X.-D. Liu, M.-Y. Luo, N.-J. Xu, Roles of physical exercise in neurodegeneration: Reversal of epigenetic clock. *Transl. Neurodegener.* **10**, 30 (2021).
26. Y.-S. Feng, S.-D. Yang, Z.-X. Tan, M.-M. Wang, Y. Xing, F. Dong, F. Zhang, The benefits and mechanisms of exercise training for Parkinson's disease. *Life Sci.* **245**, 117345 (2020).
27. Y.-H. Wang, H.-H. Zhou, Q. Luo, S. Cui, The effect of physical exercise on circulating brain-derived neurotrophic factor in healthy subjects: A meta-analysis of randomized controlled trials. *Brain Behav.* **12**, e2544 (2022).
28. S.-Y. Lin, K. Wu, E. S. Levine, H. T. J. Mount, P.-C. Suen, I. B. Black, BDNF acutely increases tyrosine phosphorylation of the NMDA receptor subunit 2B in cortical and hippocampal postsynaptic densities. *Mol. Brain Res.* **55**, 20–27 (1998).
29. A. Volianskis, G. France, M. S. Jensen, Z. A. Bortolotto, D. E. Jane, G. L. Collingridge, Long-term potentiation and the role of N-methyl-D-aspartate receptors. *Brain Res.* **1621**, 5–16 (2015).
30. X. Zhou, Q. Ding, Z. Chen, H. Yun, H. Wang, Involvement of the GluN2A and GluN2B subunits in synaptic and extrasynaptic N-methyl-D-aspartate receptor function and neuronal excitotoxicity. *J. Biol. Chem.* **288**, 24151–24159 (2013).
31. P. Calabresi, P. Gubellini, D. Centonze, B. Picconi, G. Bernardi, K. Chergui, P. Svenningsson, A. A. Fienberg, P. Greengard, Dopamine and cAMP-regulated phosphoprotein 32 kDa controls both striatal long-term depression and long-term potentiation, opposing forms of synaptic plasticity. *J. Neurosci.* **20**, 8443–8451 (2000).
32. Y. Smith, R. M. Villalba, D. V. Raju, Striatal spine plasticity in Parkinson's disease: Pathological or not? *Parkinsonism Relat. Disord.* **15**Suppl 3, S156–S161 (2009).
33. E. Ferrari, D. Scheggia, E. Zianni, M. Italia, M. Brumana, L. Palazzolo, C. Parravicini, A. Pilotto, A. Padovani, E. Marcello, I. Eberini, P. Calabresi, M. Diluca, F. Gardoni, Rabphilin-3A as a novel target to reverse  $\alpha$ -synuclein-induced synaptic loss in Parkinson's disease. *Pharmacol. Res.* **183**, 106375 (2022).
34. E. De Leonibus, F. Manago, F. Giordani, F. Petrosino, S. Lopez, A. Oliverio, M. Amalric, A. Mele, Metabotropic glutamate receptors 5 blockade reverses spatial memory deficits in a mouse model of Parkinson's disease. *Neuropsychopharmacology* **34**, 729–738 (2009).
35. E. De Leonibus, T. Pascucci, S. Lopez, A. Oliverio, M. Amalric, A. Mele, Spatial deficits in a mouse model of Parkinson disease. *Psychopharmacology (Berl)* **194**, 517–525 (2007).
36. C. Rodo, F. Sargolini, E. Save, Processing of spatial and non-spatial information in rats with lesions of the medial and lateral entorhinal cortex: Environmental complexity matters. *Behav. Brain Res.* **320**, 200–209 (2017).
37. E. Guatteo, F. R. Rizzo, M. Federici, A. Cordella, A. Ledonne, L. Latini, A. Nobili, M. T. Viscomi, F. Biamonte, K. K. Landrock, A. Martini, D. Aversa, C. Schepisi, M. D'Amelio, N. Berretta, N. B. Mercuri, Functional alterations of the dopaminergic and glutamatergic systems in spontaneous  $\alpha$ -synuclein overexpressing rats. *Exp. Neurol.* **287**, 21–33 (2017).
38. P. Calabresi, A. Pisani, N. B. Mercuri, G. Bernardi, Long-term potentiation in the striatum is unmasked by removing the voltage-dependent magnesium block of NMDA receptor channels. *Eur. J. Neurosci.* **4**, 929–935 (1992).
39. D. Mineo, F. Cacace, M. Mancini, A. Vannelli, F. Campanelli, G. Natale, G. Marino, A. Cardinale, P. Calabresi, B. Picconi, V. Ghiglieri, Dopamine drives binge-like consumption of a palatable food in experimental Parkinsonism. *Mov. Disord.* **34**, 821–831 (2019).
40. V. Bagetta, C. Sgobio, V. Pendolino, G. Del Papa, A. Tozzi, V. Ghiglieri, C. Giampà, E. Zianni, F. Gardoni, P. Calabresi, B. Picconi, Rebalance of striatal NMDA/AMPA receptor ratio underlies the reduced emergence of dyskinesia during D2-like dopamine agonist treatment in experimental Parkinson's disease. *J. Neurosci.* **32**, 17921–17931 (2012).
41. P. Calabresi, N. B. Mercuri, G. Sancesario, G. Bernardi, Electrophysiology of dopamine-denervated striatal neurons. Implications for Parkinson's disease. *Brain* **116**, 433–452 (1993).

#### Acknowledgments

**Funding:** This work was supported by grants from the Fresco Parkinson Institute to New York University School of Medicine and the Marlene and Paolo Fresco Institute for Parkinson's and Movement Disorders, which were made possible with support from Marlene and Paolo Fresco (to V.G., P.C., and A.C.); by the Italian Ministry of Education, University and Research (MIUR)–2017ENN4F; by the Italian Ministry of Health, Ricerca Corrente RC 2022 (to P.C. and B.P.); Biomarker by MUR–National Research Council (to P.C. and E.D.L.); and PNRR-MAD-2022-12375804, Italian Ministry of Health (to P.C.). **Author contributions:** P.C., B.P., E.D.L., and V.G. conceived and designed the study. F.Ca., G.M., G.N., and V.G. designed and performed electrophysiological recordings. P.C. supervised the electrophysiology experiments. M.E.C. took care of the animal ethical and health issues. F.Ca., G.M., G.N., V.G., and V.L. designed, performed, and analyzed the behavioral experiments. E.D.L. supervised the behavioral experiments. A.C., M.D.C., F.S., V.L., F.Cr., and M.T.V. designed and carried out the immunohistochemistry, immunofluorescence, DA neuron counting, and Sholl analysis experiments. M.T.V. and E.D.L. supervised these experiments. F.G. and E.F. performed the molecular analyses. P.C., V.G., F.Ca., and G.M. wrote the first draft of the manuscript. P.C. and V.G. revised the manuscript. All authors discussed the results and commented on the manuscript. **Competing interests:** The authors declare that they have no competing interests. **Data and materials availability:** All data needed to evaluate the conclusions in the paper are present in the paper and/or the Supplementary Materials.

Submitted 13 February 2023

Accepted 13 June 2023

Published 14 July 2023

10.1126/sciadv.adh1403

## Intensive exercise ameliorates motor and cognitive symptoms in experimental Parkinson's disease restoring striatal synaptic plasticity

Gioia Marino, Federica Campanelli, Giuseppina Natale, Maria De Carluccio, Federica Servillo, Elena Ferrari, Fabrizio Gardoni, Maria Emiliana Caristo, Barbara Picconi, Antonella Cardinale, Vittorio Loffredo, Francesco Crupi, Elvira De Leonibus, Maria Teresa Viscomi, Veronica Ghiglieri, and Paolo Calabresi

*Sci. Adv.*, **9** (28), eadh1403.  
DOI: 10.1126/sciadv.adh1403

### View the article online

<https://www.science.org/doi/10.1126/sciadv.adh1403>

### Permissions

<https://www.science.org/help/reprints-and-permissions>

Use of this article is subject to the [Terms of service](#)

---

*Science Advances* (ISSN ) is published by the American Association for the Advancement of Science. 1200 New York Avenue NW, Washington, DC 20005. The title *Science Advances* is a registered trademark of AAAS.  
Copyright © 2023 The Authors, some rights reserved; exclusive licensee American Association for the Advancement of Science. No claim to original U.S. Government Works. Distributed under a Creative Commons Attribution NonCommercial License 4.0 (CC BY-NC).